Laser-Produced Plasma Source System Development

Igor V. Fomenkov, David C. Brandt, Alexander N. Bykanov, Alex I. Ershov, William N. Partlo, David W. Myers, Norbert R. Böwering, Georgiy O. Vaschenko, Oleh V. Khodykin, Jerzy R. Hoffman, Ernesto Vargas L., Rodney D. Simmons, Juan A. Chavez, Christopher P. Chrobak
Cymer Inc, San Diego, CA 92127, USA

ABSTRACT

This paper describes the development of laser produced plasma (LPP) technology as an EUV source for advanced scanner lithography applications in high volume manufacturing. EUV lithography is expected to succeed 193 nm immersion technology for critical layer patterning below 32 nm beginning with beta generation scanners in 2009. This paper describes the development status of subsystems most critical to the performance to meet joint scanner manufacturer requirements and semiconductor industry standards for reliability and economic targets for cost of ownership. The intensity and power of the drive laser are critical parameters in the development of extreme ultraviolet LPP lithography sources. The conversion efficiency (CE) of laser light into EUV light is strongly dependent on the intensity of the laser energy on the target material at the point of interaction. The total EUV light generated then scales directly with the total incident laser power. The progress on the development of a short pulse, high power CO_2 laser for EUV applications is reported.

The lifetime of the collector mirror is a critical parameter in the development of extreme ultra-violet LPP lithography sources. The deposition of target materials and contaminants, as well as sputtering of the collector multilayer coating and implantation of incident particles can reduce the reflectivity of the mirror substantially over the exposure time even though debris mitigation schemes are being employed. The results of measurements of high energy ions generated by a short-pulse CO_2 laser on a laser-produced plasma EUV light source with Sn target are presented. Droplet generation is a key element of the LPP source being developed at Cymer for EUV lithography applications. The main purpose of this device is to deliver small quantities of liquid target material as droplets to the laser focus. The EUV light in such configuration is obtained as a result of creating a highly ionized plasma from the material of the droplets. Liquid tin is the material of choice to be used as a target due to the relatively high CE of the laser energy into in-band EUV radiation. Results obtained with the droplet generator and technical challenges related to successful implementation of the device are discussed.

Keywords: EUV source, EUV lithography, Laser Produced Plasma, High Volume Production

1. INTRODUCTION

LPP has many advantages over low-power discharge produced plasma (DPP) sources. The drive laser power is scalable through increasing the repetition rate and pulse energy making it easily extendable to even higher powers for future generations of EUV scanners or to compensate photoresist sensitivity limitations. The high conversion efficiency (CE) of CO_2 and Sn enables the required EUV power levels for high volume manufacturing (HVM) to be achieved at relatively low laser power so that reasonable laser costs can be realized. The isolated plasma in the central region of the source chamber provides large distances between the hot plasma and chamber components. There are no electrodes, hence there is no need for elaborate and expensive electrode cooling, nor is there any electrode debris as observed in DPP sources. The small etendue of an LPP source significantly reduces the complexity of optical system designs and supports illuminators with variable sigma and advanced illumination techniques such as annular, dipole, or quadrupole. Mass–limited usage of targets is made possible with droplet generator designs creating very small droplet diameters leading to little or no debris generation. Normal Incidence (NI) collector mirrors exhibit greater thermal load capacity and greater image fidelity under high heat load. The multi-layer (ML) coating provides substantial spectral filtering of out-of-band (OOB) EUV radiation. In addition, the ML coating can be stacked or the number of layer periods can be increased providing sacrificial layers that extend the useful lifetime of the NI collector and enable a low-cost operation of the source in a HVM environment. The goal of our development efforts is to provide a cost-effective high-power LPP EUV light source that meets all requirements for EUV lithography in production for post-193 nm technology, as described in the joint specifications of the exposure tool integrators[1].

Emerging Lithographic Technologies XI, edited by Michael J. Lercel,
Proc. of SPIE Vol. 6517, 65173J, (2007) · 0277-786X/07/$18
doi: 10.1117/12.713454

2. LPP EUV DEVELOPMENT SYSTEM

Two LPP EUV systems were built. The first system is used for the investigation and optimization of EUV radiation production and is targeting the improvement of performance parameters at low repetition rate or in single-pulse mode. A schematic of this setup is shown in Figure 1. The second system was built for system integration purposes and operation primarily at high repetition rates. This second system is described in more detail in a companion paper in these proceedings[2].

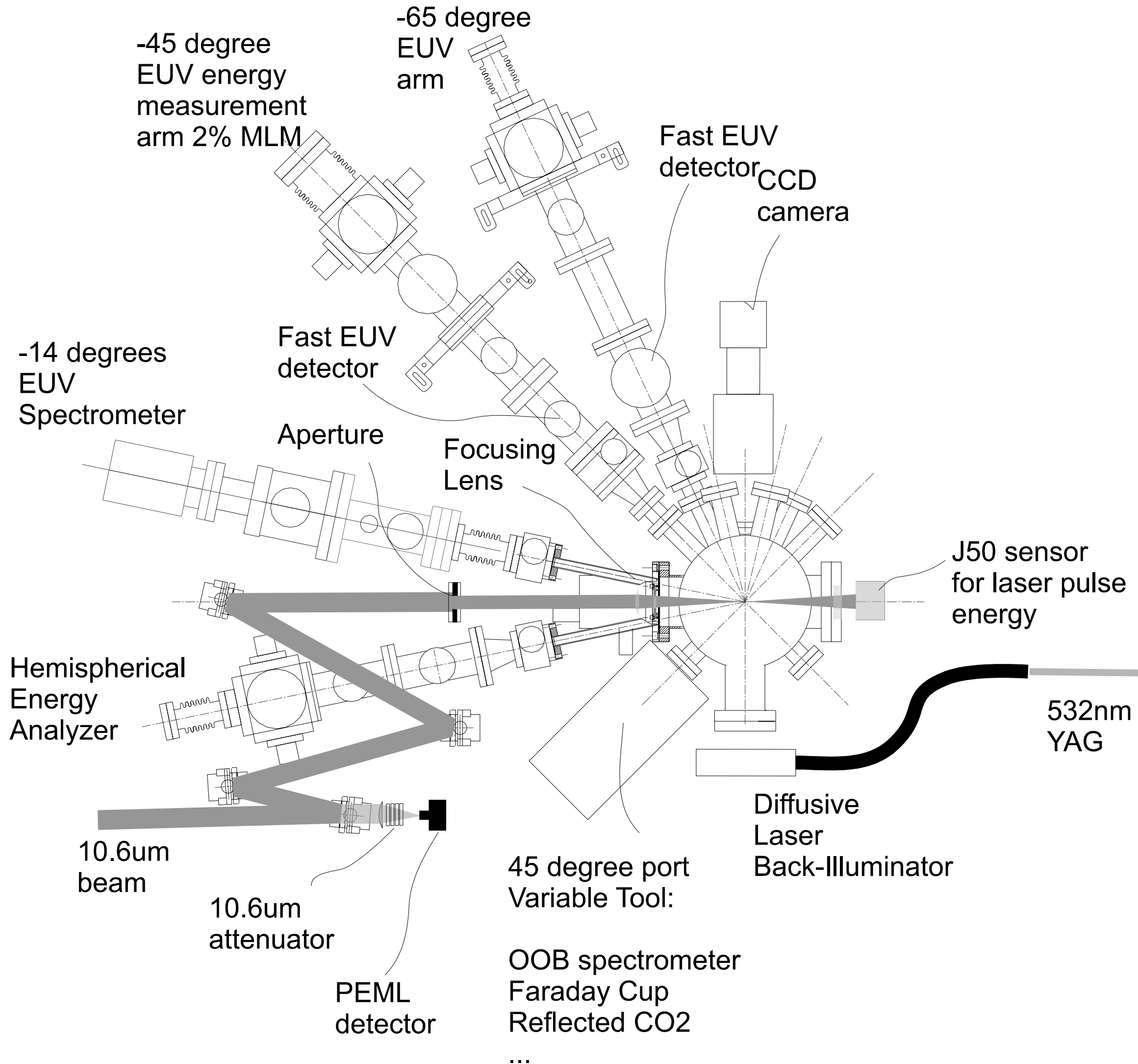

Figure 1. Experimental setup for detailed studies of the generation of EUV radiation.

The first setup was designed for maximum flexibility of the experiments and therefore equipped with numerous subsystems and diagnostic tools. The vacuum chamber was designed for installation of both flat targets and droplet generators. The permanent diagnostics includes two EUV energy measurement arms (mounted at 45 and 65 degrees with respect to the incident laser beam), an EUV spectrometer for the wavelength range from 6 - 22 nm with the capability for time-resolved measurements of spectra, and a hemispherical energy analyzer (HEA) for ion detection. The EUV measurement arms are equipped with fast EUV photodiodes for time-resolved EUV measurements and measurement of instantaneous EUV power. Back-illumination with 532 nm Nd:YAG laser light is used for shadow-

imaging of the droplets with a time resolution of better than 10 ns. The shadow-imaging tool may be installed at 90 or 45 degrees with respect to the laser beam. One version of the shadow imaging tool uses a continuous light source for back illumination in combination with a gated CCD camera (Princeton Instruments) as detector.

The port at 45 degrees is used for exchangeable diagnostics, depending on the experimental requirements. The devices that can be used here are a Faraday cup (Kimball Physics, FC-73A), OOB spectrometers with CaF_2 windows (Ocean Optics, 220-1000 nm), an IR detector (PEM-L) with ZnSe window, and an EUV pinhole camera with the capability of time-resolved measurements.

The main CO_2 laser pulse was generated by a modified Cymer laser (6000 series). The conversion included replacement of windows, modification of electrode geometry and pre-ionization, matching of the electric circuitry of the commutator, and gas mixture optimization for generation of CO_2 laser pulses. The laser configuration consisted of a master oscillator (MO) and three power amplifiers (PAs). An electro-optic crystal installed behind the MO was used for variation of the pulse length and optimization of the pulse shape. The pulse energy delivered to the target was up to 200 mJ. In addition to the main laser, two Nd:YAG lasers (10 ns and 0.15 ns with harmonic conversion of the wavelength) were employed either for back-illumination or pre-pulsing of the target at various angles with respect to the main pulse.

The energy of CO_2 laser beam was measured time-resolved with the PEM-L IR detector that was calibrated with a J-50 pyroelectric detector. A ZnSe window was used as chamber output window to measure the transmitted laser light in the case of droplet targets.

The HEA and Faraday cup were used for measurements of ions generated by the LPP. These devices are shown schematically in Figure 2a and Figure 2b. For given voltage applied to the HEA electrodes, only ions with a given E/Z ratio are transmitted. The waveform signal from the MCP detector enables to separate ions with different energy by time-of-flight measurement. Thus, the HEA provides information about ion energy and charge. For absolute measurements of the ion flux intensities, a calibration of the MCP sensitivity for the various ion energies is required.

The Faraday cup was configured for ion detection by applying a negative voltage of 50-70 V to the suppression grid to reduce the influence of secondary electrons emitted from the collector. Since the collector response is independent on the ion energy, the interpretation of data from Faraday cup is fairly straightforward: the energy of the ions is calculated from the distance to the plasma and the time-of-flight measured from the waveform; the ion flux intensity for a given energy is proportional to the voltage at a given time. The collector was loaded with a resistor of 1 kOhm.

For OOB measurements several different tools were used. Currently, spectrometers for measurements of spectra for most regions from 6 nm to 1000 nm wavelength are available. An overview for the set of tools used for OOB measurements is given in Figure 3. For the range from 6 nm to 22 nm we use a grazing-incidence spectrometer. The spectrometer sensitivity is calibrated at 13.5 nm with an absolute EUV in-band detector. The EUV in-band energy measured with the spectrometer correlates with the EUV energy detector to a high degree of accuracy. Currently, a spectrometer is being developed at Cymer for the spectral region from 20 to 200 nm. For the wavelength range from 6 nm to 70 nm thin metal foils for absolute calibration will be used. For the UV, visible and NIR regions three miniature spectrometers (Ocean Optics fiber optics spectrometers) equipped with individual fiber optics are used. The absolute sensitivity of the spectrometers was initially calibrated with a standard solar spectrum and later re-calibrated with a DH-2000-CAL calibration tool. The shortest wavelength in solar spectrum which may be used for absolute sensitivity calibration is at a wavelength of 320 nm. Employment of this calibration tool enabled us to extend our calibrated measurements down to 220 nm. A calibrated PEM-L detector was employed for measurement of reflected radiation at 10.6 μm.

Bands of high MLM reflection where the reflectivity is comparable to or exceeding those for 13.5 nm are shown on the bottom line in Figure 3 in grey color. These bands extend from 130 to 400 nm and beyond 1.5 um. OOB radiation in these bands may cause either undesirable exposure of photo-resist (for the UV-DUV range) or additional heating of the wafer and mask (in the case of the IR band).

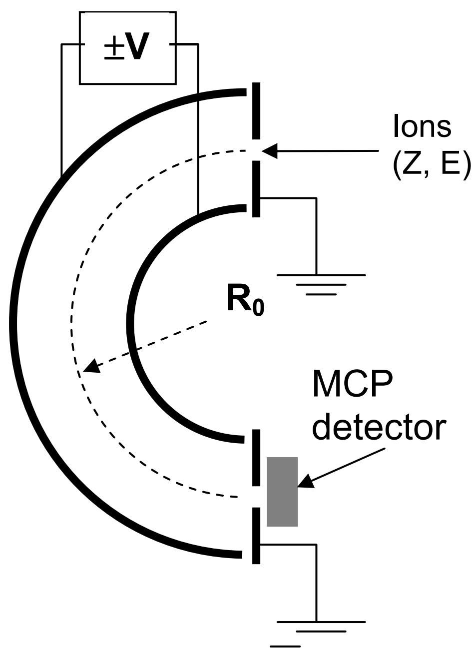

Figure 2a: Hemispherical energy analyzer for highly charged ions with MCP detector.

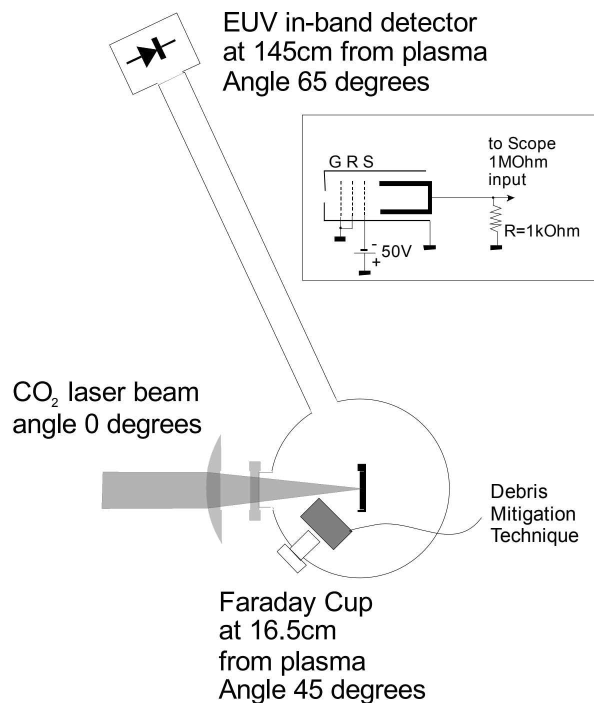

Figure 2b: Experimental configuration for detection of ion signal with Faraday cup behind debris mitigation region and for EUV detection with in-band photodiode detector.

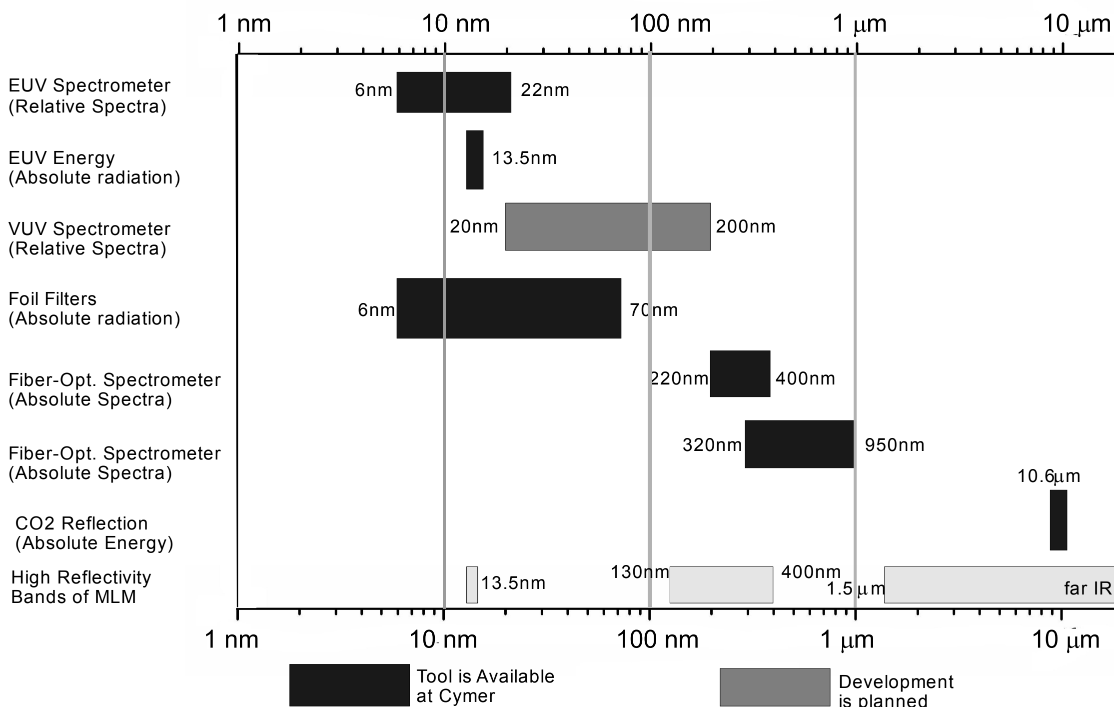

Figure 3. Spectral measurement tools (absolute and relative spectra) available at Cymer for diagnostics of the EUV light source.

3. LPP EUV EXPERIMENTAL RESULTS

The key optimization parameter is in-band EUV conversion efficiency. Previously, we have presented data for several different combinations of drive laser and target material[3]. Results of the measurements of EUV CE for Sn target and CO_2 laser are shown in Figure 4.

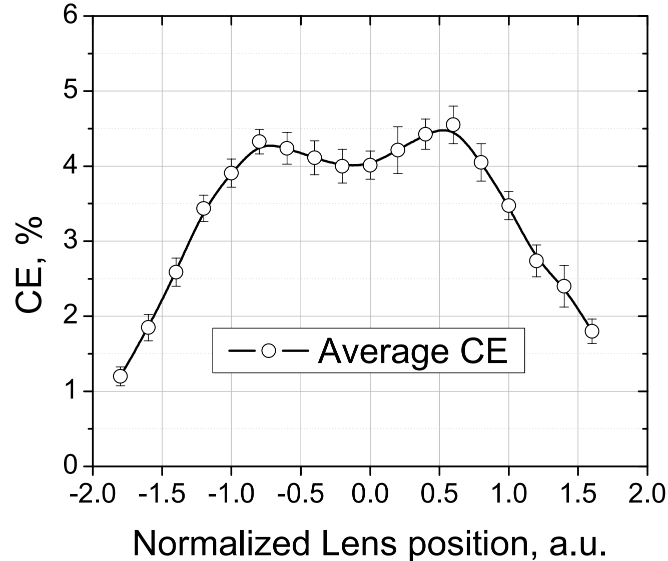

Figure 4: Average CE measured as a function of focusing lens position. Values of up to 4.5% are observed.

The pulse shape was optimized for maximum CE. The beam quality was improved such that a "double hump" feature could be observed on lens scanning curve. Measurements were conducted on flat Sn targets. Measurement results for several pulses (5-10) were averaged for providing the lens scanning curve with error bars. The observed double hump indicates that the radiation intensity is optimal at the two maxima on the curve and exceeds the optimum value at the focal point between the humps. The modeling of the dependence of CE versus laser intensity was published before[3]. The simulation shows only a small change (less than 1%) of CE when the CO_2 laser intensity is increased beyond the optimal value of 10^{10} W/cm^2. This makes it difficult to observe a very pronounced dip on the lens scanning curve in the case of 10.6 μm radiation in comparison to the case of 1.06 μm radiation where the CE drops rapidly with intensity when the optimal value is exceeded.

The measured spectra at various intensities of laser radiation confirm that the optimum plasma parameters are reached at maximum observed CE. Figure 5 shows spectra at optimal intensity (black curve) and at an intensity approximately 4 times less than optimal (gray curve) in direct comparison. The optimal spectrum matches the reflectivity curve of MLM coating of the collector (dashed line) very well, with very small OOB EUV radiation. When the laser intensity is less than optimal, the plasma temperature is less than optimal and the spectrum shifts to longer wavelengths. When the laser intensity exceeds the optimal value, the spectral emissions indicate an elevated plasma temperature above the optimal value, but this variation is less pronounced and therefore not shown in the figure.

Ions emitted from the plasma at optimal laser intensity were characterized with both HEA and Faraday cup. The measurement results are presented in Figures 6 and 7, respectively.

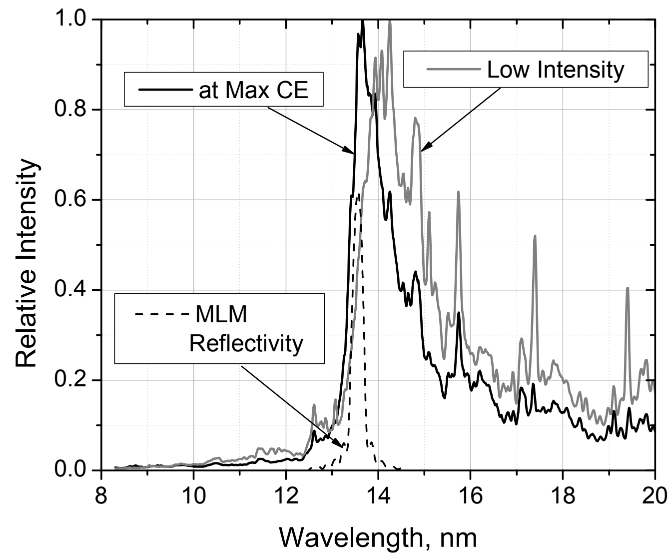

Figure 5: EUV spectra measured at optimal laser intensity (maximum CE) and at low laser intensity in comparison.

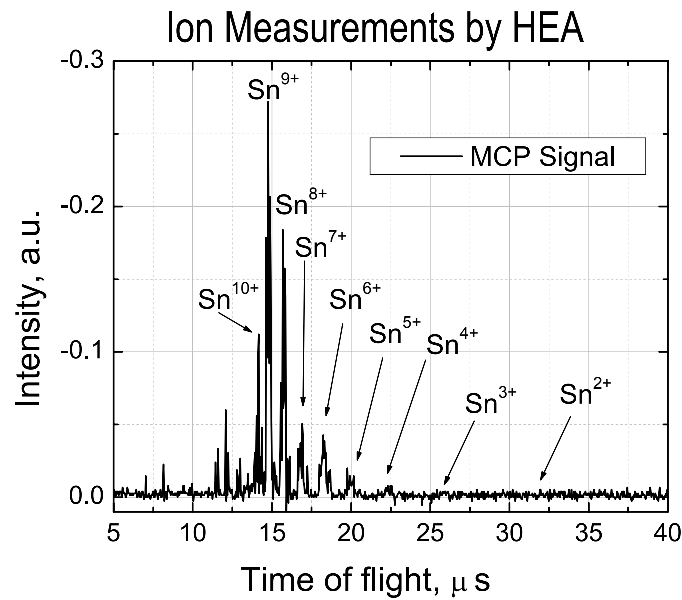

Figure 6: Sn ion time-of-flight distributions confirming that the conditions are optimized for high EUV CE.

HEA measurements show that significant number of ions originating from the plasma have a charge Z from 8 to 10. These ion states of Sn radiate photons with wavelengths close to 13.5 nm. Thus, the ion composition characterization confirms that the plasma conditions are optimal for high EUV in-band radiation.

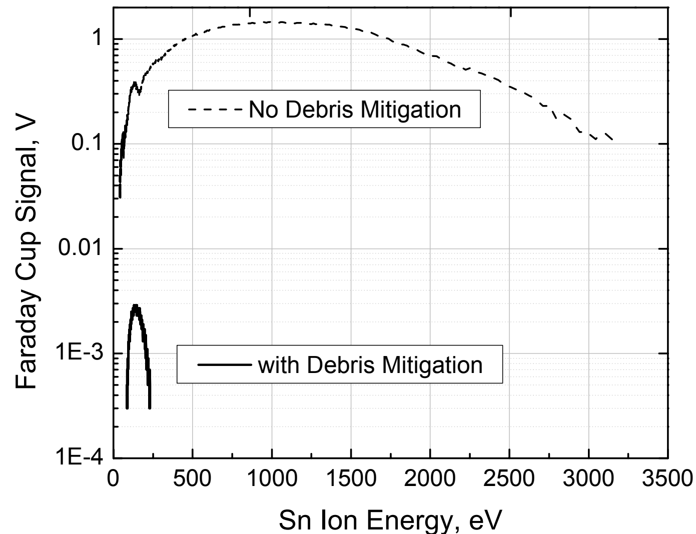

Figure 7: Ion flux measurements obtained with Faraday cup and characterization of ion flux suppression by the debris mitigation technique. With the developed debris mitigation technique the ion flux on the collector was reduced by 4 orders of magnitude and the maximum observed energy of ions dropped to <300eV. The EUV transmission is >80 %.

Faraday cup measurements show the ion intensity as a function of energy. The peak of the distribution function is at approximately at 1 keV; the highest observed energies in the spectrum were 3.0-3.2 keV. The high-energy threshold was limited by the short distance from plasma to Faraday cup (16.5 cm). Transitional relaxation processes from initial photons/electrons generate a negative spike on the waveform. Previously, the ion characterization was made at a four times larger distance to the detector such that the positive pulse of ions was distinctly separated from the initial negative spike. However, most of the ions had energies less than 3 keV for CO_2 laser intensities close to optimum for high EUV generation.

When debris mitigation was applied for ion flux attenuation, the flux was reduced by four orders of magnitude and the maximum observed energy in the spectrum was less than 300 eV with a peak value at approximately 200 eV. These results demonstrate the extremely high efficiency of the developed technique. This will mitigate the action of ions on the MLM collector significantly and achieve an economically attractive lifetime of the collector mirror coating. The transmission of the debris mitigation for EUV light was also measured and found to be more than 80 %.

UV, visible and near infrared spectra have been measured at optimal laser intensity on flat targets with the three miniature spectrometers. After calibration of the spectrometers with the solar spectrum and the DH-2000-CAL calibration tool, the spectral intensity was obtained in absolute units (μJ/nm into 2π solid angle) assuming a uniform angular distribution of the radiation. The resulting spectra are presented in Figure 8. The overlapping bands of the spectra measured with different spectrometers coincide with a high degree of accuracy.

Figure 9 shows measured spectral density versus wavelength on a semi-logarithmic plot. The blank and solid squares show measurements with using the DH-2000 and the solar spectrum for calibration. The measured values fit well to an exponential line. Extrapolation of the line to the region from 100 to 220 nm enables an estimation of the OOB radiation for this region. This shows that in the 130-400 nm band the OOB contribution from plasma is 40-70 % of the EUV in-band radiation intensity. This may imply that a spectral purity filter is required for a LPP EUV source.

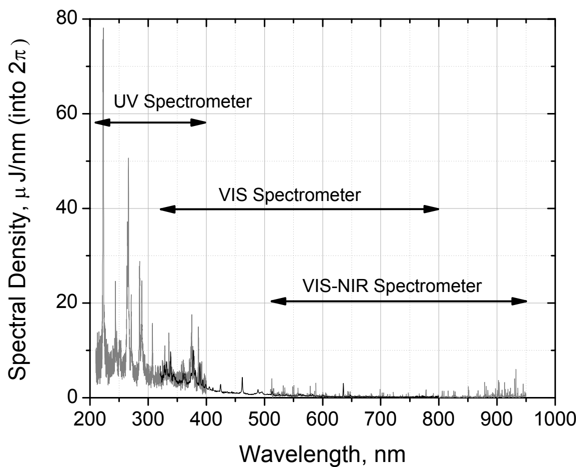

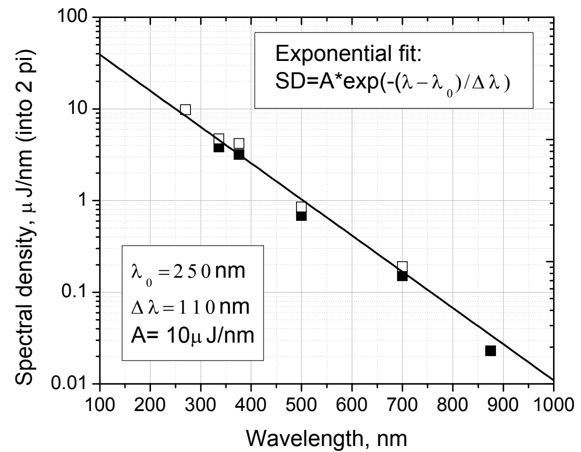

Figure 8: OOB radiation measurements extended from 950 nm down to 220 nm.

Figure 9: Extrapolation into the DUV region. It is estimated that the DUV contribution is about 40-70 % of the in-band EUV contribution.

4. DROPLET GENERATOR

The main purpose of a droplet generator is to deliver small quantities of liquid target material (droplets) to the focused spot of a high power pulsed laser. In order to achieve a high EUV power both the pump laser and the droplet generator should operate at frequencies well in excess of 10 kHz. This condition requires the liquid target material to be supplied at a 10 – 100 bar pressure. In addition, the droplet generator should be kept at a temperature exceeding the melting point of the target material. The combination of these conditions creates a significant challenge for the design of the droplet generator and limits the choice of materials that can be used in such device.

For long-term operation of the EUV source the most important parameters of the droplet generator are the spatial stability of the jet, low timing jitter of the droplets, and reliable operation that does not require any service interruptions. The spatial stability of the jet is achieved by an active steering mechanism, whereas the timing jitter is minimized by optimizing the design of the nozzle used to produce the droplets and the parameters, such as a pushing gas pressure and piezo driver voltage. The droplet generators are being systematically tested and the parameters of the droplets are evaluated using high-speed photography and optical stability measurement techniques.

Recently, a third generation droplet generator has been commissioned at Cymer. It is the result of an extensive development effort aimed at achieving reliable target delivery with characteristics tunable over a wide range[4]. The key parameters of this device can be summarized as follows: droplet frequency range: 10 – 550 kHz, droplet diameter range: 17 – 240 µm, timing jitter < 0.5 %, continuous operation time > 55 hours. Figure 10a demonstrates the capability of the new droplet generator to produce tin droplets with a wide variety of parameters. In this specific case stable droplets with 40 – 150 µm diameters were obtained in a range of frequencies of 18 – 402 kHz. This was obtained in a single run using a droplet generator equipped with a 30 µm nozzle. Using an even smaller size nozzle of 10 µm diameter, tin droplets as small as 17 µm were demonstrated at 550 kHz repetition rate. This droplet size satisfies the condition of a mass limited target, i. e., a target where each atom can be ionized and participate in the EUV emission process.

Figure 10b shows the progress that has recently been achieved in improving the timing stability of the droplets. The top figure shows a typical variation of the droplets period as a function of droplet number prior to optimization of the droplet generator parameters. The following plot demonstrates the stability improvement achieved by the optimization. A timing jitter of 120 ns (standard deviation) on a 41.6 µs period was obtained. Further stability increase is obtained by modification of the tin nozzle design. The resulting droplet stability is shown in the bottom portion of the Fig. 10b. A

timing jitter of 25 ns (0.2 % of the droplet period) was demonstrated without using any active stabilization techniques. At the plasma location this corresponds to a spatial uncertainty of the droplet arrival of ± 0.6 µm. The short term positional (transverse) stability of the droplets is on the order of 5 µm, whereas the long term (~ 15 minutes) stability is in the 100 µm range. The transverse variations of the jet position are efficiently compensated by the active stabilization steering system.

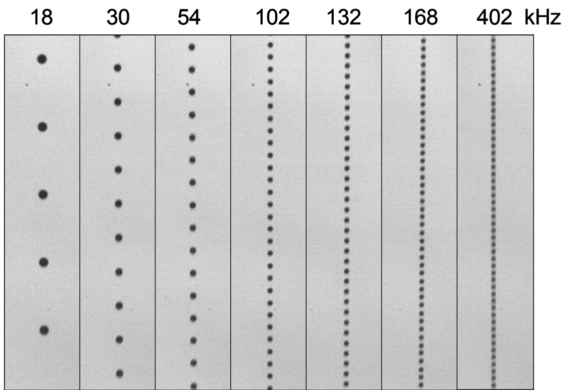

Figure 10a: Images of the tin droplets obtained in a single run of the new droplet generator with a 30 µm nozzle. With the current configuration a wide range of frequencies can be covered. The shadow images were obtained using a CCD camera with pulsed illumination.

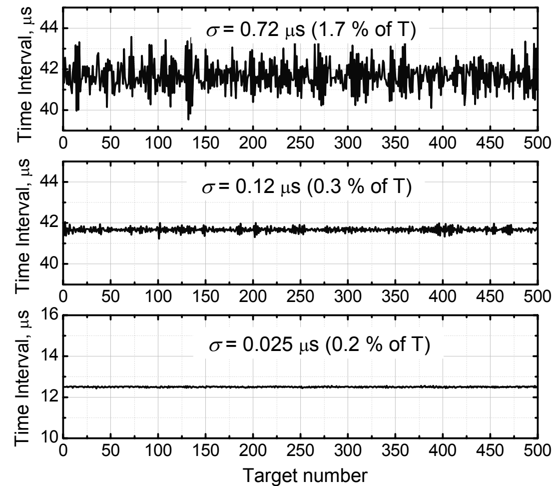

Figure 10b: Tin droplet stability diagrams showing the measured droplet-to-droplet time interval as a function of the droplet number at the plasma location. Top: droplets at 24 kHz, before optimization; middle: droplets at 24 kHz, after optimization; bottom: droplets at 80 kHz obtained with an improved nozzle design.

5. HIGH POWER CO_2 LASER

High power CO_2 drive laser has been under development for the last two years with a team made up of various CO_2 laser manufactures, university professors, and private consulting firms. Many different laser architectures were considered, however, the only one that met all of the requirements was the master oscillator, power amplifier (MOPA) configuration. A brief description of our pulsed CO_2 laser developments has been presented previously[5]. A main requirement is that the laser is not the master clock of the system. The trade off from this requirement is a decrease in laser energy stability as shown in Figure 11a. The measured energy is shown as a function of pulse number from the start of a pulse sequence. The initial ~10 pulses have a higher energy than the subsequent pulses due to the well-known gain spiking at the turn-on of the RF discharge. I addition the laser stability is expected to improve as the droplet-to-droplet stability of the generator improves.

The master oscillator (MO) of the laser system is a reliable modified commercially available unit consisting of a low-power Q-switched, RF-pumped CO_2 laser. The seed pulse from the MO is propagated nearly 50 meters through the three power amplifiers, with more than two hundred optical elements used to condition and guide the beam, before it enters the vacuum vessel to interact with the Sn droplet to produce EUV. An image of the beam taken with a Spiricon camera is shown in Figure 11b. Due to the high number of optics the beam does not have a fully Gaussian profile. The measured M^2 of the beam is approximately 2. Further improvements to the beam quality can be made by incorporating spatial filters into the beam path and by using optics with higher surface quality compared to standard CO_2 laser optics.

Figure 12 shows the initial conceptual layout for the first generation of a production-worthy CO_2 drive laser. The three power amplifiers will be arranged in an “L” shape with the master oscillator located on one of the vertical breadboards. This layout represents almost a 30% reduction in optical path length from the development system currently in use. All optics will be water-cooled and solidly mounted. Beam diagnostics will be added after each major element to monitor

the condition of the laser beam. Further product development efforts for the HVM tool are directed at reducing the footprint of the laser resonators by 50 %, and of the associated support equipment (RF generators, water heat exchangers, etc.) by 60 %.

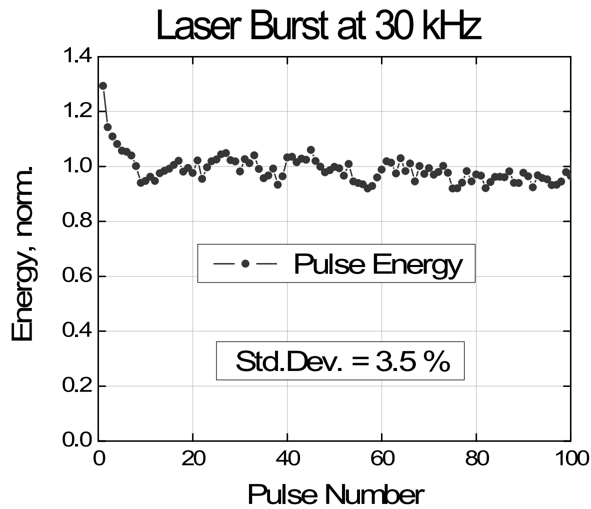

Figure 11a: The measured laser energy stability, excluding the initial startup transient, has a standard deviation of 3.5 %.

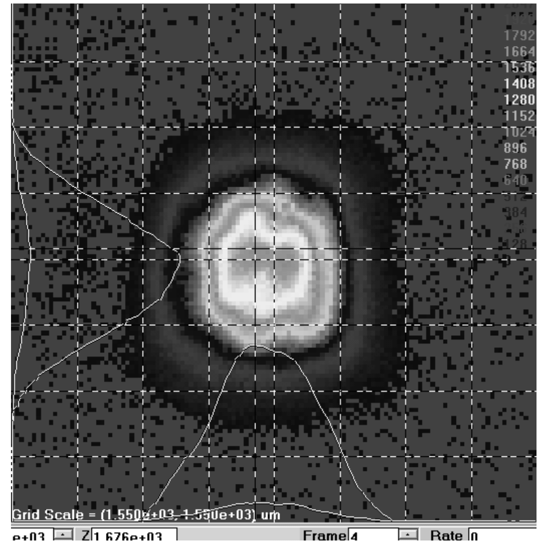

Figure 11b: Spirion image at the output of the CO_2 laser. The measured M2 value of the laser is ~2.0.

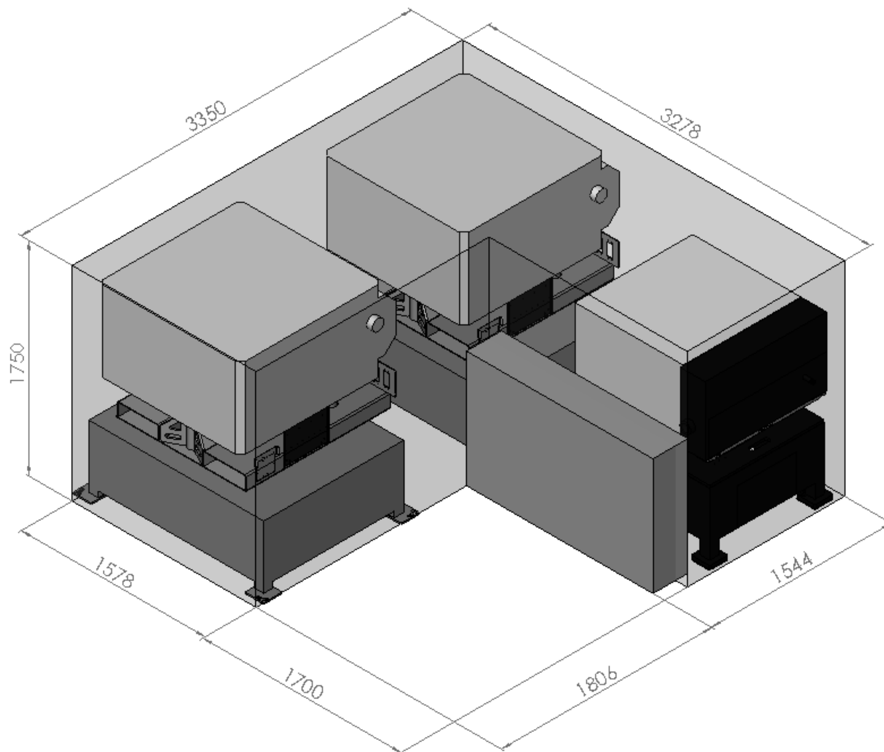

Figure 12: Conceptual drive laser design layout.

6. SUMMARY

A laser-produced plasma EUV source has been shown to be a viable source technology with high scalability to meet requirements from leading scanner manufacturers and provide a path towards higher power as the lithography tools evolve over their life cycle. EUV powers exceeding 25W at intermediate focus have been reported. An ion suppression debris mitigation technique was shown to have a measured suppression factor of 10^4 for normal-incidence collectors. The high-conversion-efficiency combination of 10.6 μm laser radiation and Sn source element has been described with CE well in the range of 3 – 4.5 %. High CE values enable the use of relatively low laser powers to provide both high EUV power and low cost to meet the needs of the chip-making industry. EUV lithography is expected to be the critical-dimension imaging solution post-193 nm immersion in 2011. LPP source technology is the most viable solution to enable the IF power requirement projected in the future and to provide the much needed margin in photoresist sensitivity, optics degradation, process latitude, and overall equipment throughput. The laser-produced plasma technology is our chosen technology path for HVM EUV lithography applications. High conversion efficiency is the key to cost effective solutions. High-power high-repetition rate CO_2 laser technology has been validated and is operational above the 6kW level.

REFERENCES

1. K. Ota, Y. Watanabe, V. Banine, H. Franken, in: "EUV Sources for Lithography", Edt. Vivek Bakshi, (SPIE Press, Bellingham, WA 2005), Chapter 2, p 27 – 43.

2 D. C. Brandt, I. V. Fomenkov, A. I. Ershov, W. N. Partlo, D. W. Myers, N. R. Böwering, A. N. Bykanov, G. O. Vaschenko, O. V. Khodykin, J. R. Hoffman, E. Vargas L., R. D. Simmons, J. A. Chavez, C. P. Chrobak, "LPP EUV Source Development for HVM", in *Emerging Lithographic Technologies XI*, edited by M. J. Lercel, Proc. of SPIE, Vol. **6517-25** (SPIE, Bellingham, WA, 2007).

3. B. A. M. Hansson, I. V. Fomenkov, N. R. Böwering, A. I. Ershov, W. N. Partlo, D. W. Myers, O. V. Khodykin, A. N. Bykanov, C. L. Rettig, J. R. Hoffman, E. Vargas L, R. D. Simmons, J. A. Chavez, W. F. Marx, and D. C. Brandt, "LPP EUV Source Development for HVM**",** in *Emerging Lithographic Technologies X*, edited by M. J. Lercel, Proc. of SPIE Vol. **6151** (SPIE, Bellingham, WA, 2006), 6151OR.

4. J. M. Algots, O. Hemberg, A. Bykanov, in: *Emerging Lithographic Technologies IX*, edited by R. S. Mackay, Proc. of SPIE Vol. **5751**, 248-259 (2005).

5. I. V. Fomenkov, B. A.M. Hansson, N. R. Böwering, A. I. Ershov, W. N. Partlo, V. B. Fleurov, O. V. Khodykin, A. Bykanov, C. L.Rettig, J. R. Hoffman, E. Vargas L., J. A. Chavez, W. F. Marx, D. C. Brandt, "High Power Low Cost Drive Laser for LPP Source", in *Emerging Lithographic Technologies X*, edited by M. J. Lercel, Proc. of SPIE Vol. **6151** (SPIE, Bellingham, WA, 2006) 61513X.